

# Explaining the Hard Excesses in AGN

D. J. Walton <sup>\*</sup>, R. C. Reis and A. C. Fabian

*Institute of Astronomy, Cambridge University, Madingley Road, Cambridge, CB3 0HA*

## ABSTRACT

A common model invoked to describe the X-ray spectra of active galaxies includes a relativistically blurred reflection component, which in some cases can be the dominant contributor to the received flux. Alternative interpretations are often based around complex absorption, and to date it has proven difficult to determine between these two viable models. Recent works on *SUZAKU* observations of the active nuclei in NGC 1365, 1H 0419-577 and PDS 456 have found the presence of strong X-ray emission at high ( $\sim 10$ -50 keV) energies, referred to as ‘hard excesses’, and it has been claimed this emission cannot be explained with simple disc reflection models. Here we investigate the high energy emission in these sources by constructing disc reflection models and show that they can successfully reproduce the observed spectra. In addition, we find the behaviour of NGC 1365 and 1H 0419-577 in these observations to be broadly consistent with previous work on disc reflection interpretations.

## Key words:

## 1 INTRODUCTION

High quality X-ray spectra of active galactic nuclei (AGN) often display complex deviations from the powerlaw continuum expected from the intrinsic X-ray source. Since the launches of the *XMM-Newton* and *Chandra* observatories in 1999, a wealth of high quality data on these spectral features in the  $\sim 0.5$ –10.0 keV energy range has been obtained, and depending on the choice of continuum, many of them can be interpreted as either emission or absorption features, with viable models having been proposed for both cases.

In the disc reflection/light bending interpretation, the fraction of the powerlaw continuum emitted in the direction of the accretion disc is reprocessed into an additional ‘reflected’ emission component. If the accretion disc extends to the innermost stable circular orbit of the black hole, the strong gravity present will cause the reflection component to appear smooth and can produce broadened and skewed emission lines. An extreme example of this behaviour is presented by Fabian et al. (2009). In this case the primary source of the intrinsic powerlaw continuum is also located in a region of strong gravity, and gravitational light bending focuses some of the emission from this component down onto the disc, providing an explanation for the spectral variability often observed; if the location of the primary source varies in distance from the central black hole, the fraction of the emitted flux focussed onto the disc, and hence that observed, also varies (see *e.g.* Miniutti & Fabian 2004). Amidst such variations, the observed spectrum can be totally dominated by the reflection component, even if the intrinsic flux of the powerlaw component has not changed.

An alternative interpretation is that the observed spectral features may arise as a result of complex absorption. The absorbing

material may be neutral, partially or almost fully ionised, and could fully cover the source or only obscure some fraction of it. In addition, the structure of the absorbing material might be complex leading to absorption by multiple layers of gas with differing physical circumstances and dimensions. For a review of the absorption processes relevant to this interpretation see Turner & Miller (2009). Possible suggestions for the origins of such gas range from the dusty torus and broad emission line region (BLR) clouds expected in the standard picture of AGN to outflowing (possibly relativistic in some cases) disc winds, so the velocity structure of the absorbing material is also important. Appropriate combinations of absorbers such as these can reproduce the observed spectra, and spectral variability is interpreted as changes in the properties of the intervening gas, *e.g.* changes in ionisation and the fraction of the intrinsic source obscured.

Despite the quality and quantity of the data provided by *XMM-Newton* and *Chandra* it has proven very difficult to distinguish between these interpretations for individual cases, a classic example being the highly variable AGN MCG-6-30-15 (see Fabian et al. 2002 and Miller et al. 2008). In July 2005 the *SUZAKU* X-ray observatory was launched, offering simultaneous X-ray observations extending up to  $\sim 70$  keV, providing potentially important broadband information against which these models can be tested. Recently, *SUZAKU* observations of NGC 1365, 1H 0419-577 and PDS 456 have revealed strong emission above 10 keV, see Risaliti et al. (2009a), Turner et al. (2009) and Reeves et al. (2009) for the respective sources. In each case, the authors claim that reflection models cannot account for this strong emission, dubbing the high energy emission ‘hard excesses’, and argue the most likely interpretation is the presence of a Compton thick ( $N_H \gtrsim 10^{24}$ – $10^{25}$  atom  $\text{cm}^{-2}$ ), partially covering absorber.

Here we construct disc reflection models and show that they can indeed account for the strong emission above 10 keV in these

<sup>\*</sup> E-mail: dwalton@ast.cam.ac.uk

sources. §2 details our data reduction, while §3 presents our spectral analysis, and in §4 we discuss our results.

## 2 OBSERVATIONS AND DATA REDUCTION

NGC 1365, 1H0419-577 and PDS 456 were observed with *SUZAKU* (Mitsuda et al. 2007) in January 2008, July 2007 and February 2007 respectively. The following sections detail our data reduction for the X-ray imaging spectrometers (XIS, Koyama et al. 2007) and the hard X-ray detector (HXD, Takahashi et al. 2007).

### 2.1 XIS Reduction

There are four XIS detectors on board *SUZAKU*, XIS0, XIS2 and XIS3 are front illuminated, and XIS1 is back illuminated, however XIS2 experienced a charge leak in November 2006 and has not been in operation since. Using the latest HEASOFT software package we processed the unfiltered event files for each of the XIS CCDs and editing modes (all observations analysed used both 3x3 and 5x5 editing modes) operational in the respective observations, following the *SUZAKU* Data Reduction Guide<sup>1</sup>. We started by creating new cleaned event files by re-running the *SUZAKU* pipeline with the latest calibration, as well as the associated screening criteria files. XSELECT was used to extract spectral products from these event files, and responses were generated for each individual spectrum. The spectra and response files for all the front-illuminated instruments operational were combined using the FTOOL ADDASCASPEC, and rebinned by a factor of 4. Finally, spectra were grouped to a minimum of 20 counts per energy bin with GRPPHA to allow the use of  $\chi^2$  minimization during spectral fitting. In this work, we only make use of the front illuminated spectra. Quoted uncertainties on model parameters are the 90 per cent confidence intervals for one parameter of interest, and the uncertainties on count rates are at the  $1\sigma$  level.

### 2.2 PIN Reduction

For the HXD PIN detector we again reprocessed the unfiltered event files for the respective observations following the data reduction guide. Since the HXD is a collimating rather than an imaging instrument, estimating the background requires individual consideration of the non X-ray instrumental background (NXB) and cosmic X-ray background (CXB). The appropriate response and NXB files were downloaded for the respective observations<sup>2</sup>; in each case the tuned (Model D) background was used. Common good time intervals were obtained with MGTIME which combines the good times of the event and background files, and XSELECT was used to extract spectral products. Dead time corrections were applied with HXDDTCOR, and the exposures of the NXB spectra were increased by a factor of ten, as instructed by the data reduction guide. The contribution from the CXB was simulated using the form of Boldt (1987), with the appropriate normalisation for the nominal pointing (all observations were performed with XIS nominal pointing), resulting in a CXB rate of  $\simeq 0.026 \text{ count s}^{-1}$ . The NXB and CXB spectra were then combined using MATHPHA to give a total background spectrum, to which a 2% systematic uncertainty was also added. Finally the data were grouped to have a

minimum of 500 counts per energy bin to improve statistics, and again allow the use of  $\chi^2$  minimization during spectral fitting.

This reduction procedure was then verified using the recently released PIN reduction script HXDPINXBPI<sup>3</sup>. The two methods were always in excellent agreement.

### 2.3 Specific Source Details

Here we provide additional details on the data reduction specific to each source.

*NGC 1365*: for this observation, XIS0, XIS1 and XIS3 were all in operation. Source spectra were extracted from circular regions of 174" radius centred on the point source, and background spectra from another region of the same size, devoid of any obvious contaminating emission, elsewhere on the same chip. The PIN data reduction yielded a source rate of  $(11.9 \pm 0.2) \times 10^{-2} \text{ count s}^{-1}$  which is 17.8 per cent of the total observed flux, and the good exposure times yielded were 161 and 137 ks for each front illuminated XIS CCD and the PIN detector respectively. The reduction performed here is in excellent agreement with that of Risaliti et al. (2009a).

*1H0419-577*: here only XIS0 and XIS3 were in operation. In addition to the usual standard filtering, we excluded XIS data with earth elevation angles  $< 10^\circ$  and a cut-off rigidity  $> 6 \text{ GeV}$  in order to match the reduction procedure adopted in Turner et al. (2009). Source and background regions were also circular regions of radius 174" and were chosen in the same manner as for NGC 1365. In this case the source was found to contribute 15.0 per cent of the total observed flux, with the source rate  $(9.4 \pm 0.2) \times 10^{-2} \text{ count s}^{-1}$ . The good exposure times yielded were 179 and 143 ks for each XIS CCD and the PIN detector respectively. Again, our reduction is in good agreement with that of Turner et al. (2009).

*PDS 456*: XIS0, XIS1 and XIS3 were again in operation for this observation. Source and background regions were chosen in the same manner as for NGC 1365, the source region was circular and of radius 174", while the background was extracted from various circular regions scattered around the CCD. The PIN detection of PDS 456 was much weaker than for the other two sources, only contributing 2.1 per cent of the observed flux, with a source rate of  $(1.2 \pm 0.2) \times 10^{-2} \text{ count s}^{-1}$  (considering only the 15.0–50.0 keV energy range, the observed rate is  $(0.6 \pm 0.2) \times 10^{-2} \text{ count s}^{-1}$ ). The good exposure times here were 190 and 165 ks for each front illuminated XIS CCD and the PIN detector respectively. The PIN rates obtained here are noticeably different from those presented in Reeves et al. (2009), with their background rate significantly lower. To further test our data reduction in this instance, we also compare the NXB model with the spectrum obtained during earth occultation (excluding earth elevation angles  $> -5^\circ$ ), another method for estimating the instrumental background, and find only a 0.4% difference between the two. Given our reduction has also been verified with HXDPINXBPI, we take our background rate to be the correct one.

## 3 SPECTRAL ANALYSIS

In order to draw attention to the spectral features present in these sources, we initially modelled the spectra with a powerlaw continuum, modified by Galactic absorption, over the 2.0–4.0 and 7.0–

<sup>1</sup> <http://heasarc.gsfc.nasa.gov/docs/suzaku/analysis/>

<sup>2</sup> <http://www.astro.isas.ac.jp/suzaku/analysis/hxd/>

<sup>3</sup> <http://heasarc.nasa.gov/docs/suzaku/analysis/pinbgd.html>

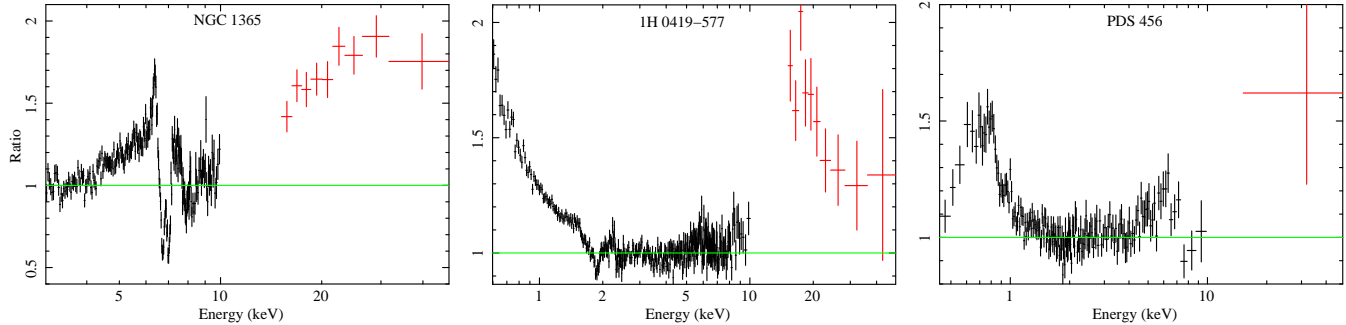


**Figure 1.** Data/model ratio plots of *SUZAKU* XIS (front illuminated; black) and PIN (red) spectra for (left to right) NGC 1365, 1H 0419-577 and PDS 456 to a powerlaw continuum model, as described in the text. Each of the sources displays strong emission above 10 keV which previous authors have claimed cannot be produced using simple reflection models alone. The data shown have been re-binned for plotting purposes only.

10.0 keV energy ranges where the intrinsic continuum may be expected to dominate the observed spectrum in a reflection interpretation. In the case of NGC 1365, Wang et al. (2009) have demonstrated that below  $\sim 2$  keV the X-ray spectrum is dominated by diffuse thermal emission using the excellent spatial resolution of *Chandra*. As such, throughout this work we only study the spectrum above 3 keV in this source, where the contribution from the diffuse emission is negligible. Figure 1 shows the data/model ratios to the powerlaw continuum for each of the three sources; note that at all times a cross calibration constant of 1.16 is applied between the XIS and PIN spectra, as recommended by the HXD calibration team<sup>4</sup>. All sources show broad, possibly skewed emission lines close to  $\sim 6.4$  keV (rest frame), and the ratio spectra of 1H 0419-577 and PDS 456 also show excess smooth emission at soft energies ( $\lesssim 2$  keV). Both of these are expected from reflection from an accretion disc extending to within a few gravitational radii ( $R_G = GM/c^2$ ) of the central black hole, where strong gravitational redshifts blur and distort the reflected emission (see *e.g.* Fabian et al. 1989, Crummy et al. 2006, *etc.*). There are also absorption like features seen at  $\sim 2$  keV in the ratio plots of 1H 0419-577 and PDS 456, but these are probably due to uncertainties in the calibration around the instrumental silicon K edge, so in all further analysis we exclude 1.7–2.1 keV from our modelling.

In addition, it is plain to see that each source displays fairly strong emission above 10 keV. At these energies, reflection models predict a broad hump of emission due to the interplay within the reflecting medium between Compton down-scattering of high energy photons and photoelectric absorption of low energy photons, a feature commonly referred to as the ‘Compton hump’. However, Risaliti et al. (2009a), Turner et al. (2009) and Reeves et al. (2009) have recently claimed that the high energy emission in these sources cannot be reproduced using simple reflection models (albeit in the case of PDS 456 with a higher PIN source rate than obtained here). In the forthcoming analysis we make use of the self-consistent reflection model REFLIONX (Ross & Fabian 2005), which intrinsically includes iron K-shell absorption and emission, to show that disc reflection interpretations can in fact successfully model this emission. The key parameters of REFLIONX are the iron abundance,  $A_{Fe}$ , the photon index of the intrinsic powerlaw continuum,  $\Gamma$ , and the ionisation parameter of the reflecting medium,  $\xi = L/nR^2$ . All models include photoelectric absorption at the

Galactic value for each source, and where necessary we also include a neutral absorption component at the redshift of the respective galaxies to account for possible additional absorption local to the source.

### 3.1 NGC 1365

We construct a model based around a disc reflection interpretation for the spectrum of NGC 1365, with the primary components being the intrinsic powerlaw continuum and a reflected component from a partially ionised accretion disc, modelled with REFLIONX. The effects of strong gravity expected in the innermost regions of the disc are accounted for by applying the KDBLUR convolution model, which makes use of the calculations of Laor (1991), to the ionised reflection component. KDBLUR assumes a powerlaw form for the emissivity profile of the accretion disc, *i.e.*  $\epsilon(r) \propto r^{-q}$ , where the emissivity index  $q$  is a free parameter; the other free parameters are the inner and outer radius and the inclination of the accretion disc,  $R_{in}$ ,  $R_{out}$  and  $i$  respectively. In addition to the broad residuals apparent in Fig. 1, there are also narrow features present in the spectrum; four absorption lines can be seen between  $\sim 6.7$ – $8.3$  keV, and there is also a further narrow iron emission line at  $\sim 6.4$  keV. The narrow emission line most likely arises due to reflection from more distant material, *e.g.* gas in the BLR and/or the dusty torus, so we also include a neutral reflection component, modelled with REFLIONX (without KDBLUR). The photon index and iron abundance were required to be the same for the separate model components, and the redshifts of the reflectors were fixed at that of the host galaxy ( $z = 0.0055$ ; de Vaucouleurs et al. 1991). The absorption lines have been studied in detail by Risaliti et al. (2005) who identify them with Fe XXV and Fe XXVI  $K\alpha$  and  $K\beta$  absorption. Such absorption lines are expected to arise due to highly ionised material which would primarily contribute narrow features, so initially we simply included four Gaussian absorption lines in order to obtain estimates for the photon index and iron abundance. Using these, we generated a photoionisation model for the absorption using XSTAR v2.2.0, in order to simultaneously account for all four lines with a single, highly ionised absorber. The free parameters of this absorption model are the column density, ionisation parameter, iron abundance and outflow velocity of the absorbing medium; for consistency we require that the iron abundance of the disc and the ionised absorber are the same.

In terms of the physical components included, the model constructed is very similar to that used in Risaliti et al. (2009a) and Risaliti et al. (2009b), the main difference being the self-consistent

<sup>4</sup> <http://www.astro.isas.jaxa.jp/suzaku/doc/suzakumemo/suzakumemo-2008-06.pdf>

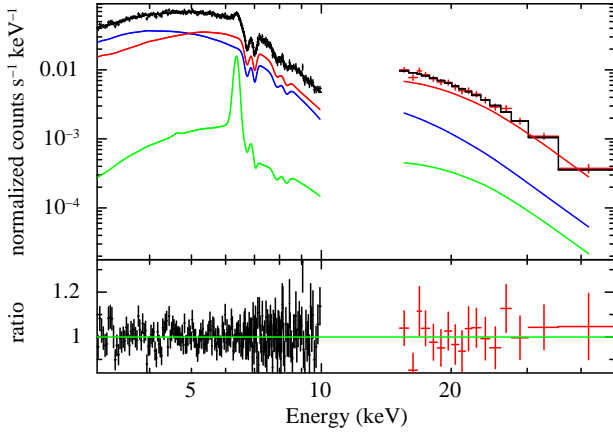


**Figure 2.** The front illuminated XIS and PIN spectra of NGC 1365, and the data/model ratios to our best fit reflection models (see text). The top panel shows the relative contributions of the powerlaw continuum (blue), disc reflection (red) and neutral reflection (green) components, with the overall model in black. The data have been re-binned for display purposes only.

treatment of the line and continuum components in the reflection spectrum provided by REFLIONX. During the spectral fitting we find that the outer radius of the accretion disc is not well constrained, so we freeze this parameter at  $400R_G$ , the maximal value allowed by KDBLUR. This model provides an excellent fit to the data, with  $\chi^2_\nu = 278/268$ , parameters are listed in Table 1, and the fit to the spectrum is shown in Fig. 2, with the relevant contributions of the various components highlighted. Notably, the model does not have any problem reproducing the data above 10 keV.

### 3.2 1H 0419-577

Here we also begin with a two component disc reflection model, as for NGC 1365. The photon index is again required to be the same for all the model components, the redshift of the reflection is fixed at the value of the host galaxy ( $z = 0.104$ ; Thomas et al. 1998), and the outer radius of the disc fixed at  $400R_G$ . This model provides a good representation of the data with  $\chi^2_\nu = 423/436$ , and importantly fits the PIN data well. However, there are still some residual features in the XIS spectrum. To resolve these we adopt the approach used in Fabian et al. (2005) when modelling *XMM-Newton* spectra of this source, and allow the emissivity index and ionisation parameter of the disc to have a radial dependence. Although a crude implementation, splitting the disc into an inner and outer region, separated by some break radius  $R_{br}$ , improves the fit by  $\Delta\chi^2 = 18$  for 4 extra degrees of freedom. An F-test finds the probability of such improvement being coincidental to be only 0.09%, so we adopt this model as our best fit. Again, the key parameters are listed in Table 1, and the fit to the spectrum is shown in Fig. 3.

### 3.3 PDS 456

Similarly to 1H 0419-577 and NGC 1365, we model the spectrum of PDS 456 with a two component powerlaw plus disc reflection interpretation. As previously stated, we allow for neutral absorption in excess of the Galactic value, however in this instance Behar et al. (2010) find the excess absorption is located at  $z = 0$ , so we allow the local absorption to vary with a lower limit of the Galactic value.

**Table 1.** Model parameters obtained through modelling the *SUZAKU* spectra of NGC 1365, 1H 0419-577 and PDS 456 with a disc reflection interpretation (see text). Parameter values marked with a \* have not been allowed to vary.

|                             | NGC 1365                | 1H 0419-577             | PDS 456                   |
|-----------------------------|-------------------------|-------------------------|---------------------------|
| $N_{H(G)}$ <sup>a</sup>     | 0.134*                  | 0.2*                    | $2.3^{+0.3}_{-0.2}$       |
| $N_{H(z)}$ <sup>a</sup>     | $95 \pm 5$              | -                       | -                         |
| $N_{H(i)}$ <sup>a</sup>     | $113^{+7}_{-11}$        | -                       | $7^{+5}_{-2}$             |
| $\xi_i$ <sup>b</sup>        | $4830^{+550}_{-800}$    | -                       | $3140^{+2980}_{-140}$     |
| $v_i$ <sup>c</sup>          | $-3120 \pm 320$         | -                       | $-96600^{+33000}_{-5000}$ |
| $\Gamma$                    | $2.01 \pm 0.04$         | $2.12 \pm 0.02$         | $2.35^{+0.05}_{-0.03}$    |
| $A_{Fe}$ <sup>d</sup>       | $2.5 \pm 0.2$           | $1.3 \pm 0.2$           | $> 8.6$                   |
| $i$                         | $57^{+3}_{-2}$          | $53 \pm 2$              | $70^{+3}_{-2}$            |
| $R_{in}$ <sup>e</sup>       | $1.85 \pm 0.15$         | $1.4 \pm 0.1$           | $< 2.0$                   |
| $R_{out}$ <sup>e</sup>      | 400*                    | 400*                    | 400*                      |
| $\xi_{inner}$ <sup>b</sup>  | $10^{+32}_{-7}$         | $92^{+50}_{-32}$        | $55^{+10}_{-3}$           |
| $\xi_{outer}$ <sup>b</sup>  | -                       | $1.1^{+0.7}_{-0.1}$     | -                         |
| $q_{inner}$                 | $5.0^{+1.0}_{-0.5}$     | $> 8.7$                 | $5.5^{+2.0}_{-1.2}$       |
| $q_{outer}$                 | -                       | $5 \pm 1$               | -                         |
| $R_{br}$ <sup>e</sup>       | -                       | $2.4 \pm 0.3$           | -                         |
| $\chi^2_\nu$                | 283/277                 | 405/432                 | 421/381                   |
| $F_{0.5-10.0}$ <sup>f</sup> | $12.78^{+0.66}_{-0.83}$ | $32.36^{+0.12}_{-0.13}$ | $6.98^{+0.03}_{-0.04}$    |
| $R_{0.5-10.0}$ <sup>g</sup> | $0.23^{+0.16}_{-0.03}$  | $0.67^{+0.23}_{-0.35}$  | $0.15^{+0.06}_{-0.04}$    |

<sup>a</sup> Column densities are given in  $10^{21}$  atom  $\text{cm}^{-2}$

<sup>b</sup> Ionisation parameters, given in  $\text{erg cm s}^{-1}$

<sup>c</sup> Outflow velocities of the ionised absorber, with respect to the host galaxy, given in  $\text{km s}^{-1}$

<sup>d</sup> The iron abundances are quoted relative to the solar value

<sup>e</sup> Radii are given in units of the gravitational radius,  $R_G = GM/c^2$

<sup>f</sup> Observed 0.5–10 keV fluxes, given in  $10^{-12}$   $\text{erg cm}^{-2} \text{s}^{-1}$

<sup>g</sup> 0.5–10 keV disc reflection fractions

The photon index is the same for the intrinsic and reflected components, the redshift of the reflection fixed at that of the host galaxy, ( $z = 0.184$ ; Torres et al. 1997) and the outer disc radius fixed at  $400R_G$ . In addition, we also include two absorption lines to model the narrow lines at 7.67 and 8.13 keV identified by Reeves et al. (2009). As with the absorption lines in NGC 1365, the absorbing material is expected to be highly ionised, so we adopted the same procedure and initially modelled them with Gaussian absorption lines to obtain estimates of the photon index and iron abundance, then used these to generate a photoionisation absorption model using XSTAR. The free parameters for this absorption model are the same as that generated for NGC 1365, and again we require that the accretion disc and the absorbing medium have the same iron abundance. This reflection-based model provides a good fit to the observed spectrum, with  $\chi^2_\nu = 414/379$ . As shown in Fig. 4, the high energy data are well modelled, as is the strong emission feature at  $\sim 0.8$  keV (see Fig. 1), identified here with iron L-shell emission, as in Reeves et al. (2009). Model parameters are listed in Table 1.

## 4 DISCUSSION AND CONCLUSIONS

With the advent of the *SUZAKU* X-ray observatory, and the HXD instrument on board, observations of sources displaying strong emission above 10 keV have come to light. The most prominent examples to date are NGC 1365, 1H 0419-577 and PDS 456, for



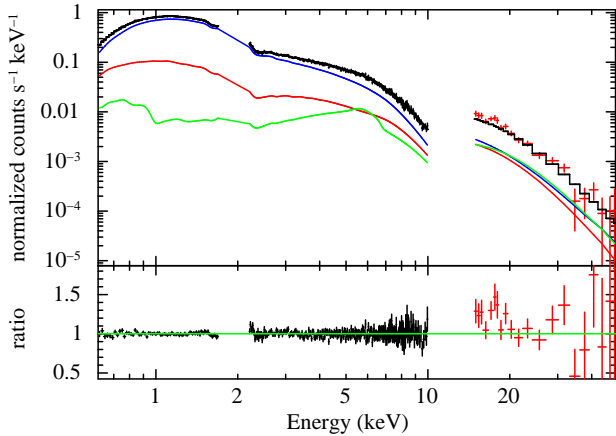


**Figure 3.** As in Fig. 2 but now for 1H0419-577. Here, the red and green components are the emission from the inner and outer regions of the accretion disc. Again, the data have been re-binned for display purposes only.

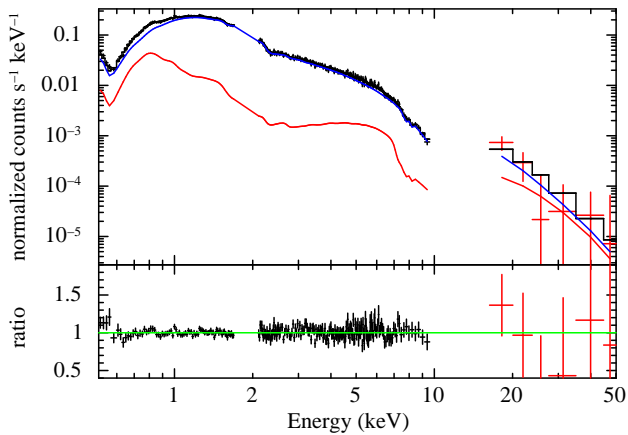


**Figure 4.** As in Figs. 2 and 3, but now for PDS 456. Again, the data have been rebinned for display purposes only.

which Risaliti et al. (2009a), Turner et al. (2009) and Reeves et al. (2009) have respectively claimed that the high energy emission is too strong to be explained with reflection models alone. In each case the emission is described as a ‘hard excess’ and interpreted as observational evidence for the presence of a partially covering, Compton thick absorber. We have investigated these claims by constructing models based on disc reflection for each of these sources to test whether they truly cannot reproduce the observed high energy spectra.

The main conclusion of this work is that for each of the sources analysed, as shown in Figs. 2, 3 and 4, disc reflection models can successfully reproduce the observed data above 10 keV, disputing the previous claims to the contrary. It must be stressed that this does not rule out the presence of Compton thick, partially covering absorbers in these sources, indeed complex absorption remains a viable alternative interpretation to the observed spectra; we are demonstrating that disc reflection can reproduce the broadband data without commenting in depth on the absorption interpretation. The reasons we have been able to fit such models to the data where the previous authors could not differ for each source. In the case of NGC 1365 the model constructed is physically very

similar to that used in Risaliti et al. (2009a), but here the reflection components are modelled with REFLIONX which self-consistently includes the reflected continuum and line features, rather than treating the two separately. In addition, the PEXRAV/PEXRIV models (Magdziarz & Zdziarski 1995) used in Risaliti et al. (2009a) as the reflection continuum components display a much stronger iron absorption edge at 7.1 keV than REFLIONX, which may also contribute to an underprediction at higher energies. For 1H0419-577 it is not clear how the modelling procedures differ, but we may have considered a broader parameter range than Turner et al. (2009). Finally, in the case of PDS 456 we find that the total background count rate obtained in Reeves et al. (2009) to be significantly lower than that obtained here, which has been verified via a variety of methods (see §2). Such underestimation of the background rate would artificially inflate the PIN spectrum with respect to the XIS data.

In their analysis of the short term variability within one of the *XMM-Newton* observations of NGC 1365, Risaliti et al. (2009b) propose a disc reflection interpretation modified by variable absorption, perhaps due to eclipsing BLR clouds. Since the model proposed here is very similar, it is not surprising we obtain some similar results, e.g. the iron abundance is  $\sim 3$  times solar, and the majority of the emission comes from within a few  $R_G$ . This new model can easily be incorporated into a scenario with such variable absorption, and a similar time resolved analysis would be useful to disentangle the curvature in the time averaged spectrum due to the broad iron line and variations in absorption. Given the spectrum obtained with the long *XMM-Newton* observation (see Risaliti et al. 2009c), the absorption does seem to vary on long time scales, though there may still be other interpretations for the short term variability. The iron abundance obtained is in excellent agreement with that found for the ring of star formation  $\sim 1.3$  kpc from the nucleus, but the more distant diffuse emission requires a sub-solar abundance ( $\lesssim 0.4$  solar; Wang et al. 2009, Guainazzi et al. 2009), so it would appear the metallicity in NGC 1365 has some radial dependence. Although the general agreement of our model with that of Risaliti et al. (2009b) is good, the disc inclination obtained here is significantly higher, and is closer to that expected for an obscured AGN in the classical unified theory (Antonucci 1993).

Using XSTAR, the absorption lines present in NGC 1365 and PDS 456 have been successfully modelled as being due to highly photoionised material. The absorption systems in these two sources have been studied in detail by Risaliti et al. (2005) and Reeves et al. (2009) respectively, including considerations of the possible origins of the absorbing material. Our modelling is broadly consistent with the previous work of these authors, and as we are interested primarily in the continuum we do not embark on any lengthy discussion of these features. There are some differences in the column densities obtained in both cases, but these are due to our requirement that the absorbers have the same iron abundance as the accretion discs; in both cases we find iron to have a super-solar abundance, while the previous work on these absorbers assumed solar abundances.

The flux of 1H0419-577 during the *SUZAKU* observation presented here shows the source to be in a high flux state according to the nomenclature used in Fabian et al. (2005), in which a light-bending interpretation is presented for the spectral variability observed across a number of *XMM-Newton* observations. In this interpretation, 1H0419-577 displays an anti-correlation between flux and reflection fraction, with which the low reflection fraction and high flux observed here is consistent. In their model, Fabian et al. (2005) also include an edge component to model OVII absorption, and note that the depth of the edge also displays an anti-correlation

with flux. No such absorption is required here, but this is consistent with the observed trend as the flux is higher than in any *XMM-Newton* observation. The iron abundance obtained here is not consistent with the previous work, since this is not expected to vary with time these observations should be revisited with this in mind. By the same nature, a similar multi-mission analysis to that performed by Behar et al. (2010) is required for the previous observations of PDS 456 to test whether the disc reflection model presented here remains acceptable. The iron abundance obtained in our analysis of this source is high, which is a consequence of the observed iron K and L-shell emission features (see Fig. 1). In this respect, PDS 456 may be similar to 1H 0707-495 (Fabian et al. 2009, Zoghbi et al. 2010). A brief inspection of the *XMM-Newton* observation taken in the same year (although not simultaneously) shows a tentative hint of an emission feature at  $\sim 0.8$  keV in the *EPIC*-pn spectrum, but there are no narrow features in the RGS spectrum, so if the same feature is present it must be fairly smooth and broad.

The inclination obtained from our spectral fit to PDS 456 is higher than would be expected for an unobscured nuclei in the unified scheme for AGN, and like the iron abundance is also primarily driven by the detection of iron L-shell emission. Lawrence & Elvis (2010) present a geometric model of the inner regions of galactic nuclei which attempts to reproduce the observed fraction of obscured AGN. The model involves the misalignment of the inner regions of the accretion disc with the obscuring material, expected to be the outer regions of the disc and the structures beyond, such as the dusty torus *etc.* In the context of PDS 456, with this model it is possible that the structures responsible for the obscuration are warped away from the line of sight. The inclination obtained from modelling the X-ray spectrum is that of the innermost regions of the accretion disc; if the outer regions are warped away from our line of sight in this source, it becomes possible to reconcile this high inclination for the inner disc with the fact that PDS 456 is an unobscured quasar. Multi-wavelength studies of a few nearby galaxies in which such substructure could be resolved do seem to hint that misalignments may be present (*e.g.* NGC 4151, NGC 1068 and Cygnus A; see §4.4 in Lawrence & Elvis 2010 for a summary of the observations). An alternative explanation comes from the possible evolution in the relative numbers of type 1 and 2 sources with luminosity seen in X-ray studies of AGN (see *e.g.* Hasinger (2008), although Lawrence & Elvis (2010) argue that this may not be the case). There appear to be fewer type 2 sources at higher X-ray luminosities, which suggests that the opening angle of the obscuring material increases with X-ray luminosity. PDS 456 is one of the brightest low redshift quasars known, and although the observation analysed here finds the source with the lowest flux to date it is still emitting at an intrinsic rest frame luminosity of  $L_{0.5-10.0} \sim 10^{45}$  erg s $^{-1}$ . If the proposed evolution of the absorber geometry with luminosity is real, PDS 456 could have a very wide opening angle and may still be seen as an unobscured quasar despite its high inclination. There are a number of other AGN which, whilst being unobscured, also require a high inner disc inclination from spectral fitting, *e.g.* Ark 120, NGC 7213 and NGC 7469 in the sample of Nandra et al. (2007), so any model for the inner regions of galactic nuclei must somehow be able to incorporate such sources.

## ACKNOWLEDGEMENTS

DJW and RCR acknowledge the financial support provided by STFC, and ACF thanks the Royal Society. The authors would also like to thank the referee for his/her useful comments.

## REFERENCES

- Antonucci R., 1993, *ARA&A*, 31, 473  
 Behar E., Kaspi S., Reeves J., Turner T. J., Mushotzky R., O'Brien P. T., 2010, *ApJ*, 712, 26  
 Boldt E., 1987, in IAU Symposium, Vol. 124, A. Hewitt, G. Burbidge, & L. Z. Fang, ed, *Observational Cosmology*, p. 611  
 Crummy J., Fabian A. C., Gallo L., Ross R. R., 2006, *MNRAS*, 365, 1067  
 , 1991, Roman d. V. G. d. V. A. C. H. G. J. B. R. J. P. G. . F. P., N. G., ed, *Third Reference Catalogue of Bright Galaxies*  
 Fabian A. C., Miniutti G., Iwasawa K., Ross R. R., 2005, *MNRAS*, 361, 795  
 Fabian A. C., Rees M. J., Stella L., White N. E., 1989, *MNRAS*, 238, 729  
 Fabian A. C. et al., 2002, *MNRAS*, 335, L1  
 Fabian A. C. et al., 2009, *Nat*, 459, 540  
 Guainazzi M., Risaliti G., Nucita A., Wang J., Bianchi S., Soria R., Zezas A., 2009, *A&A*, 505, 589  
 Hasinger G., 2008, *A&A*, 490, 905  
 Koyama K. et al., 2007, *PASJ*, 59, 23  
 Laor A., 1991, *ApJ*, 376, 90  
 Lawrence A., Elvis M., 2010, *ArXiv e-prints*  
 Magdziarz P., Zdziarski A. A., 1995, *MNRAS*, 273, 837  
 Miller L., Turner T. J., Reeves J. N., 2008, *A&A*, 483, 437  
 Miniutti G., Fabian A. C., 2004, *MNRAS*, 349, 1435  
 Mitsuda K. et al., 2007, *PASJ*, 59, 1  
 Nandra K., O'Neill P. M., George I. M., Reeves J. N., 2007, *MNRAS*, 382, 194  
 Reeves J. N. et al., 2009, *ApJ*, 701, 493  
 Risaliti G., Bianchi S., Matt G., Baldi A., Elvis M., Fabbiano G., Zezas A., 2005, *ApJ*, 630, L129  
 Risaliti G. et al., 2009a, *ApJ*, 705, L1  
 Risaliti G. et al., 2009b, *ApJ*, 696, 160  
 Risaliti G. et al., 2009c, *MNRAS*, 393, L1  
 Ross R. R., Fabian A. C., 2005, *MNRAS*, 358, 211  
 Takahashi T. et al., 2007, *PASJ*, 59, 35  
 Thomas H., Beuermann K., Reinsch K., Schwobe A. D., Truemper J., Voges W., 1998, *A&A*, 335, 467  
 Torres C. A. O., Quast G. R., Coziol R., Jablonski F., de La Reza R., Lepine J. R. D., Gregorio-Hetem J., 1997, *ApJ*, 488, L19  
 Turner T. J., Miller L., 2009, *A&A Rev.*, 17, 47  
 Turner T. J., Miller L., Kraemer S. B., Reeves J. N., Pounds K. A., 2009, *ApJ*, 698, 99  
 Wang J., Fabbiano G., Elvis M., Risaliti G., Mazzarella J. M., Howell J. H., Lord S., 2009, *ApJ*, 694, 718  
 Zoghbi A., Fabian A. C., Uttley P., Miniutti G., Gallo L. C., Reynolds C. S., Miller J. M., Ponti G., 2010, *MNRAS*, 401, 2419